Unsteady Diffusion in Ternary Gas Mixtures

K. R. ARNOLD and H. L. TOOR

Carnegie Institute of Technology, Pittsburgh, Pennsylvania

Unsteady diffusion in the system methane-argon-hydrogen was studied in a Loschmidt apparatus with large changes in concentration. The mean concentration-time history was predicted within experimental error by the linearized equations of multicomponent mass transfer. In the calculations the Stefan-Maxwell equations were used to obtain the diffusivity matrix which was evaluated at the equilibrium concentration.

Digital computer solutions to the nonlinear differential equations were also obtained for various systems and boundary conditions. The fluxes predicted by the linearized equations with the diffusivity matrix evaluated at the arithmetic average of the initial and boundary concentrations were in all cases within 5% of the numerical predictions.

The linearized theory of multicomponent mass transfer assumes that the elements of the diffusivity matrix in the basic transport equation

$$(\mathrm{j}) = -[D]\, C \nabla (y) \tag{1}$$

may be taken as independent of concentration. Successful numerical tests of this assumption showed that the fluxes predicted in this manner were in close accord with predictions of the Stefan-Maxwell equations. These tests were carried out on ternary gas systems with steady state unidirectional diffusion (*9*) and with steady state transfer in a boundary layer (*8*).

This paper describes additional unsteady state tests in ternary gas mixtures. It includes experimental studies in a bounded system of a nature which have not been carried out heretofore, as well as numerical studies of the nonlinear diffusion equations in both bounded and unbounded systems.

For isothermal, isobaric systems with no external forces, the Stefan-Maxwell equations for mixtures of ideal gases invert to Equation (1) with $[D]$ given in terms of the $\mathcal{D}_{ij}$ and concentration (*11*). For a three-component system a 2×2 matrix may be used and its elements are given by (*9, 10*).

$$\begin{aligned} D_{11} &= \mathcal{D}_{13}\,[\mathcal{D}_{23}\, y_1 + \mathcal{D}_{12}\,(1 - y_1)]/S \\ D_{22} &= \mathcal{D}_{23}\,[\mathcal{D}_{13}\, y_2 + \mathcal{D}_{21}\,(1 - y_2)]/S \\ D_{12} &= y_1\, \mathcal{D}_{23}\,(\mathcal{D}_{13} - \mathcal{D}_{12})/S \\ D_{21} &= y_2\, \mathcal{D}_{13}\,(\mathcal{D}_{23} - \mathcal{D}_{21})/S \\ S &= y_1\, \mathcal{D}_{23} + y_2\, \mathcal{D}_{13} + y_3\, \mathcal{D}_{12} \end{aligned} \tag{2}$$

The two roots of the matrix are real and non-negative (*9*).

To examine the effect of the concentration dependence of $[D]$ with a minimum complication, work was carried out with $\mathbf{V}^M = 0$ and with unidirectional transfer. In addition C is constant and there is no chemical reaction in this work, so combination of Equation (1) with the continuity equations yields (*10*)

$$\frac{\partial (y)}{\partial \theta} = \frac{\partial}{\partial z}[D]\frac{\partial (y)}{\partial z} \tag{3}$$

The experimental study used a Loschmidt type of diffusion apparatus (*6*): two vertical tubes of length L, each filled with gas at a uniform concentration, are brought together at time zero and interdiffusion is allowed to take place. The boundary conditions are

$$\begin{aligned} &\theta < 0,\ 0 < z < L\ ,\ (y) = (y^+) \\ &\theta < 0,\ -L < z < 0,\ (y) = (y^-) \\ &\theta > 0,\ z = \pm L\ ,\ \frac{\partial (y)}{\partial z} = (0) \end{aligned} \tag{3a}$$

The temperature and pressure are constant, there is negligible volume change on mixing, and natural convection is not to be expected. Hence for constant molar density, the overall continuity equation gives

$$\frac{\partial V_z^M}{\partial z} = 0 \tag{4}$$

and since $V_z^M = 0$ at $z = \pm L$, $V_z^M = 0$ everywhere as assumed in writing Equation (3).

With $[D]$ assumed to be constant, we have a simplified example of the linearized equations for which the general solution is

$$(y - y^-) = [F]\,(y^+ - y^-) \tag{5}$$

For a ternary system the elements of the 2×2 $[F]$ matrix are given by (*10*)

$$F_{ij} = \frac{D_{ij} - D_2\delta_{ij}}{D_1 - D_2} F(D_1) + \frac{D_{ij} - D_1\,\delta_{ij}}{D_2 - D_1} F(D_2), \qquad i, j = 1, 2 \tag{5a}$$

For this situation $F(D_k)$ is described by

$$F(D_k) = \frac{1}{2}\left[1 \pm \frac{2}{\pi}\sum_{n=0}^{\infty}\frac{1}{m}\sin\frac{m\pi z}{L}\exp\left\{-\left(\frac{m\pi}{L}\right)^2 D_k\,\theta\right\}\right] \tag{5b}$$

where $m = n + \frac{1}{2}$.

The length average concentration from $z = -L$ to 0 is given by

$$(\tilde{y} - y^-) = [F]\,(y^+ - y^-) \tag{6}$$

and $[F]$ is now given by Equation (5*a*), with (5*b*) replaced by

$$F(D_k) = \frac{1}{2} - \frac{1}{\pi^2}\sum_{n=0}^{\infty}\left(\frac{1}{m}\right)^2 \exp\left\{-\left(\frac{m\pi}{L}\right)^2 D_k\,\theta\right\} \tag{6a}$$

K. R. Arnold is at Shell Research and Development Company, Emeryville, California.

The multicomponent penetration solution was also used. Here the boundary conditions on Equation (3) are ($V_z{}^M$ at $z = \infty$ is assumed to be zero, so as before $V_z{}^M = 0$ everywhere)

$$\begin{array}{lll} \theta < 0 \ , & z > 0 \ , & (y) = (y^o) \\ z = \infty \ , & & (y) = (y^o) \\ z = 0 \ , & \theta > 0 \ , & (y) = (y^I) \end{array} \qquad (7)$$

and the solution is

$$(y - y^o) = [F]\,(y^I - y^o) \qquad (8)$$

where $[F]$ is given by Equation (5*a*), but here

$$F(D_k) = 1 - \text{erf}\frac{z}{2\sqrt{D_k\,\theta}} \qquad (8a)$$

The flux across the boundary is given by

$$(N^I) = [F]\,C\,(y^I - y^o) \qquad (9)$$

and again $[F]$ is given by Equation (5*a*), but in this case

$$F(D_k) = \sqrt{\frac{D_k}{\pi\,\theta}} \qquad (9a)$$

This solution was given earlier (9) in another form.

It can be seen from Equation (2) that if the three binary diffusion coefficients are equal, the cross coefficients D_{ij}, $i \neq j$ are zero and the main coefficients D_{ii} are independent of composition. Hence at this limit each component diffuses (with respect to the molar average velocity) as if it were in a binary mixture, and the interactions are zero. As the differences among the binary diffusion coefficients increase (increasing differences among molecular weights of the three components), Equation (2) shows that the cross coefficients increase relative to the main coefficients and both the cross and main coefficients become more concentration dependent. Hence, in order to obtain large interactions and large variations in the D_{ij}, the system hydrogen-argon-methane was chosen and large concentration differences were used. This system severely tests the linearized equations.

EXPERIMENTAL PROCEDURE

The apparatus consisted of two diffusion cells (four diffusion tubes), and temperature control, vacuum, and analysis systems. The diffusion cells were operated independently but their construction was integrated into one unit. The 1/2-in. diameter constant bore glass tubes were mounted on brass plates drilled so that the top and bottom tubes were aligned into a single diffusion path when the plates were in one position and closed to one another when in a second position. The surfaces of the plates were lapped to provide a vacuum seal when they were properly lubricated. The plates were also fitted with small diameter glass tubes to load and unload the tubes with gas samples. A second glass tube was placed around each diffusion tube, forming an annular section. Water at 34.00 ± 0.01°C. was circulated through the annular sections for temperature control. The entire apparatus was in an air bath controlled to ± 0.2°C.

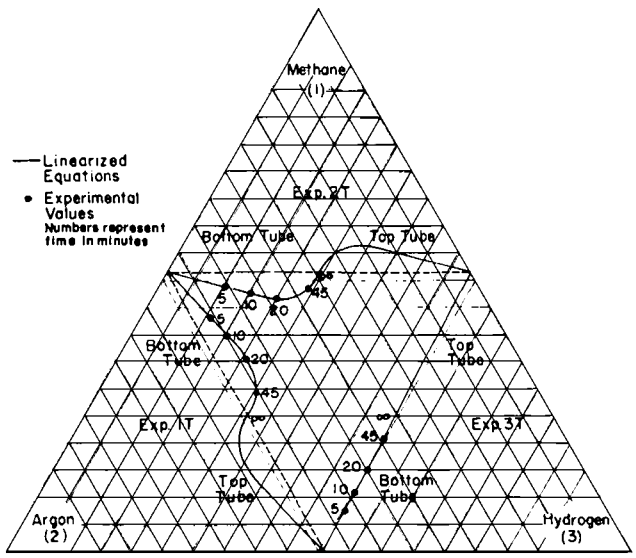

Fig. 1. Concentration paths. Numbers on curves represent the time in minutes from the start of a run.

Pure gases as well as binary mixtures were obtained from Matheson and Company. The compositions of the mixtures were determined by the manufacturer and also on both the gas chromatograph used for the run analysis and on a mass spectrometer. The results of these analyses were within ½ mole % of one another.

After evacuation of the system, the diffusion tubes were loaded with the desired gas mixtures and a run started by aligning the tubes. After a specified time the tubes were separated, the contents were mixed, and the mixtures in the bottom tubes were analyzed on a Beckman GC2 gas chromatograph. Three to five repeated analyses were made on each sample; the results were generally within 0.5 mole % of the mean. Pure methane and hydrogen were used for calibration and argon was obtained by difference.

Table 1. Binary Diffusivities (Sq. Ft./Hr.)

	Experimental	Literature	Standard deviation
Hydrogen-methane	2.99°	2.99 (3)	0.03
Hydrogen-argon	3.23	3.24 (2)	0.05
Argon-methane	0.836	—	0.008

° Length chosen to fit literature value.

RESULTS AND DISCUSSION

Before studying the ternary system, runs were made on the three binary pairs. This was done, not only as a check of the experimental system, but to determine cell constants, the lengths of the diffusion tubes. They were determined from the binary solution corresponding to Equation (5):

$$\frac{\tilde{y} - y^-}{y^+ - y^-} = F(\mathcal{D}_{kj}) \qquad (10)$$

with F given by Equation (6*a*). The twenty-one hydrogen-methane diffusion runs were used. The best literature value (3) of $\mathcal{D}_{H_2-CH_4}$ corrected to the experimental temperature and pressure was used to give a value of $(\pi/L)^2 = 5.85$ ft.$^{-2}$ for cell *A* and $(\pi/L)^2 = 5.57$ ft.$^{-2}$ for cell *B*. These values fell within 1% of the measured lengths. The run times for the above determination were varied from 5 to 20 min. A slight variation of L (or more properly $\mathcal{D}_{kj}$) with run time was observed, but this variation fell within the expected experimental error. Using the above values of L, we calculated the experimental binary

Table 2. Initial Conditions, Mole Fraction

Experiment No.	Top tube Methane	Top tube Hydrogen	Bottom tube Methane	Bottom tube Hydrogen
1*T*	0.0	0.491	0.515	0.0
2*T*	0.448	0.512	0.515	0.0
3*T*	0.448	0.512	0.0	0.491

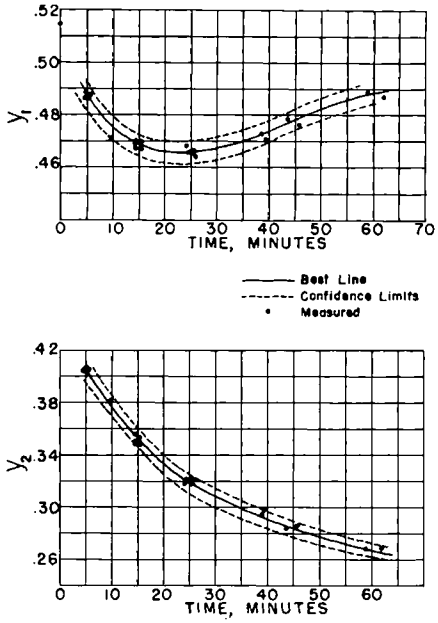

Fig. 2. Concentration vs. time, experiment 2T.

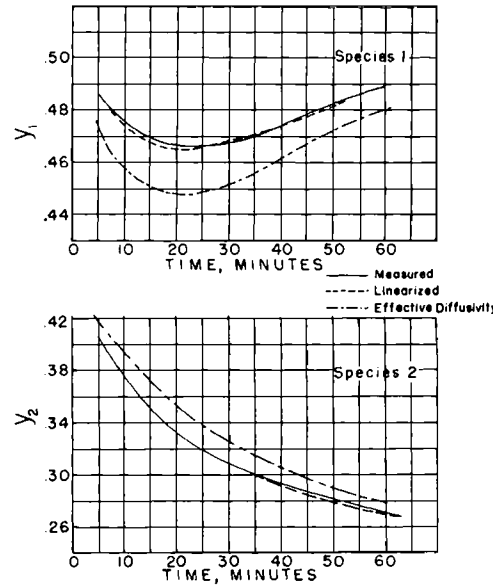

Fig. 3. Concentration vs. time, experiment 2T; comparison of experiment with predictions.

diffusivities and standard deviations from the mean value; they are shown in Table 1.

Experimental values were also obtained for the binary diffusion coefficients for the remaining two pairs, hydrogen-argon and methane-argon. As seen in Table 1, $\mathcal{D}_{H_2-A}$ agrees favorably with the literature value. A reliable independent experimental value for $\mathcal{D}_{CH_4-A}$ is not known to the authors.

The ternary data were divided into three experiments, 1*T*, 2*T*, and 3*T*, depending upon the initial conditions. As shown in Table 2 the initial compositions in the tubes were binary mixtures paired such that there were maximum initial composition differences for two components, hereafter called the *active components*, and a near zero initial concentration difference for the third, the *inactive component*.

The run times were varied from 5 to 60 min. during which time radical composition changes occurred within the tubes. This is seen on a ternary composition diagram (Figure 1) where the composition paths are shown for the three experiments. The data points are average values estimated from the complete set, while the solid lines are the predictions of the linearized theory [Equation (6)]. On this scale the two cannot be distinguished. The dotted lines show paths which would be followed if there were no interactions.

It can be seen from Figure 1 that in all three experiments the denser mixture was initially in the bottom half of the tube and in all but 1*T* the mean density in the bottom half of the tube was always greater than the mean density in the top half. Since no anomalies appeared in experiment 1*T*, natural convection apparently did not set in to any significant extent.

Experiments 1*T* and 2*T* are similar in that large interactions are present. The cross-diffusion coefficients D_{12} and D_{21} are similar in magnitude to the main coefficients D_{11} and D_{22}. By contrast, the cross coefficients for run 3*T* are small, since the active components, argon and methane, have roughly the same diffusivities with respect to hydrogen, the inactive component. Thus small interactions were expected and found experimentally. In Figure 2 the concentrations for experiment 2*T* are shown as a function of time. The time scale was corrected slightly for local atmospheric conditions at the time of the run and also for the cell constant; thus all twenty-one runs could be shown on one figure. The corrected time scale is given by

Cell *A*

$$\theta_{corr} = \theta \frac{760}{P}$$

Cell *B*

$$\theta_{corr} = \theta \frac{760}{P} \left(\frac{L_A}{L_B}\right)^2$$

where P is atmospheric pressure in mm. of Hg. The solid line is a best line fitted through the data by the least squares fit to a polynomial, while the broken lines are 95% confidence limits based on the standard deviation of the data from the polynomial. The reproducibility of the data

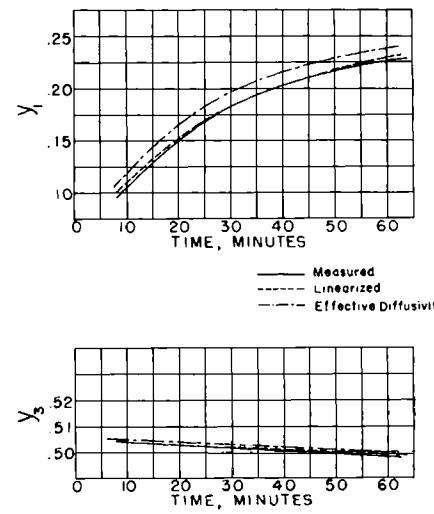

Fig. 4. Concentration vs. time, experiment 3T; comparison of experiment with predictions.

TABLE 3. [*D*] MATRIX AT INITIAL COMPOSITIONS, EXPERIMENT 2*T*

Top tube		Bottom tube	
2.99	1.69	1.99	1.15
0	1.28	1.12	1.95

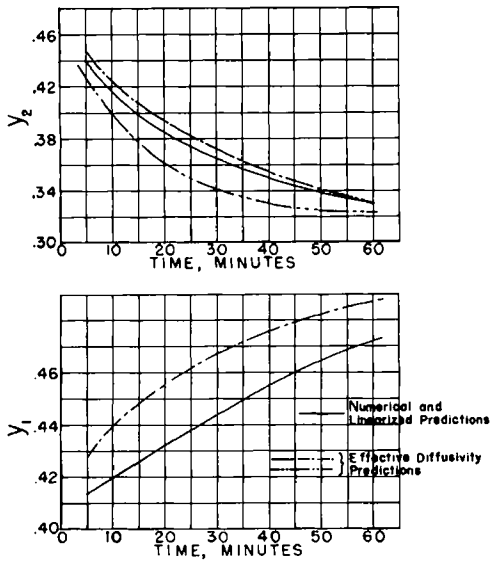

Fig. 5. Concentration vs. time, experiment *BL2*; comparison of various methods.

for runs $1T$ and $3T$ was similar to that shown for $2T$ and the confidence limits were estimated to be the same.

A comparison of the experimental results, the predictions of the linearized equations, and the predictions of an effective diffusivity method are given in Figures 3 and 4. The results of experiments $2T$ and $3T$ are shown since they represent the extremes of large and small interactions. Experiment $1T$ was similar to $2T$ (except that species 1 and 2 are interchanged).

The calculated results shown in Figures 3 and 4 were obtained by the two approximations mentioned above. The linearized predictions were made with Equation (6). The matrix $[D]$ for these calculations was evaluated at the arithmetic average of the initial top and bottom tube compositions. This average composition does not change with the run time and is the equilibrium composition. The $[D]$ matrix corresponding to the initial compositions is given in Table 3 for experiment $2T$. Even though there is a significant difference between these two matrices, it can be seen in Figure 3 that the linearized solution fits the measurements within experimental error.

The values based on an effective diffusivity cannot be calculated without ambiguity. For example, if in experiment $2T$ methane is chosen as either component 1 or 2, the predicted concentration curve will be very close to constant, regardless of which effective diffusivity is used. This is a result of a near zero concentration difference for methane, and is contrary to the experimental data. On the other hand, if methane is chosen as component 3 and argon and hydrogen as components 1 and 2, the methane concentrations may be obtained by difference. The curve obtained in this manner follows the experimental data in a qualitative manner.

The effective diffusivity used for the predictions was that proposed by Wilke (*12*) and used by Fairbanks and Wilke (*5*) for unsteady evaporation:*

$$\mathcal{D}_k = (1-\tilde{y}_k) \Big/ \sum_{\substack{j=1 \\ j\neq i}}^{n} \tilde{y}_j/\mathcal{D}_{kj} \qquad (11)$$

The concentrations at any time were then obtained by using the binary diffusion equation [Equation (10)] with the binary diffusivity replaced by $\mathcal{D}_k$. It is seen in Figure 3 that the linearized equations give a better prediction than the best of the above-mentioned effective diffusivity calculations.

The effective diffusivity given by Equation (11) was originally developed for the diffusion of a single component through a mixture of stagnant gases (*12*), so perhaps it is not surprising that difficulties were encountered in applying it to the present situation. However, ambiguities are inherent in the technique itself and the results presented here, while not exhaustive, do emphasize the ad hoc nature of the effective diffusivity method.

In experiment $3T$ the interaction effects are quite small, there is very little motion of the inactive species, and the system reduces to a pseudo binary diffusion problem with two gases acting together as a single component. The effective diffusivity model predicts a concentration dependence similar to that found experimentally, as shown in Figure 4. The predictions made by the linearized theory are again well within experimental error.

On the basis of the agreement between the experimental data and the linearized theory, one can conclude that the linearized theory gives a very good approximation to the diffusing system when the diffusivity matrix is evaluated at the average composition, even with large interactions and large changes in the concentration.

Table 4. Binary Diffusivities (Sq. Ft./Hr., 1 Atm. Pressure)

System	Species 1	2	3	$\mathcal{D}_{12}$	$\mathcal{D}_{13}$	$\mathcal{D}_{23}$
1	Nitrogen-carbon dioxide-hydrogen, 35°C.			0.705	2.81	3.50
2	Isopropanol-methanol-water, 95°C.			0.422	0.623	0.938
3	Benzene-acetone nitrogen, 35°C.			0.146	0.346	0.397

NUMERICAL SOLUTIONS

Further insight can be gained by consideration of the nonlinear equations. These were solved numerically for a number of examples and the results compared with experiment and with the results of the linearized equations. Equation (3) written out is

$$\frac{\partial y_1}{\partial \theta} = \frac{\partial}{\partial z} D_{11} \frac{\partial y_1}{\partial z} + \frac{\partial}{\partial z} D_{12} \frac{\partial y_2}{\partial z} \qquad (12a)$$

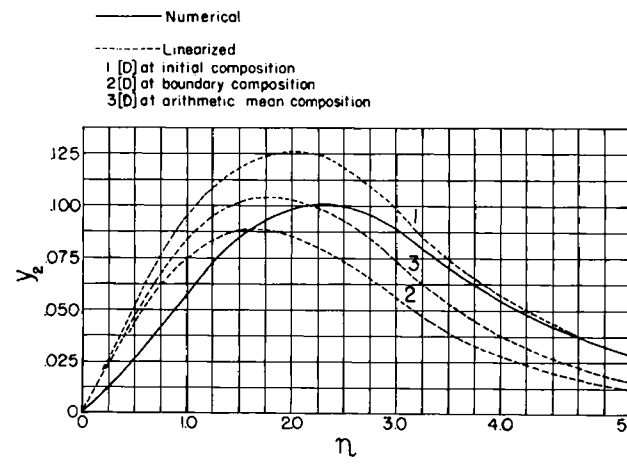

Fig. 6. Concentration profile for component 2 in Semi-infinite system.

* Fairbanks and Wilke (*5*) showed that this effective diffusivity satisfactorily described the unsteady state evaporation of a dilute component into a mixture of two gases. The solution to the linearized evaporation problem is given by Cussler and Lightfoot (*4*) and in a less cumbersome form by Arnold (*1*). When the evaporating component is dilute, the linearized solutions give essentially the same result as the effective diffusivity method.

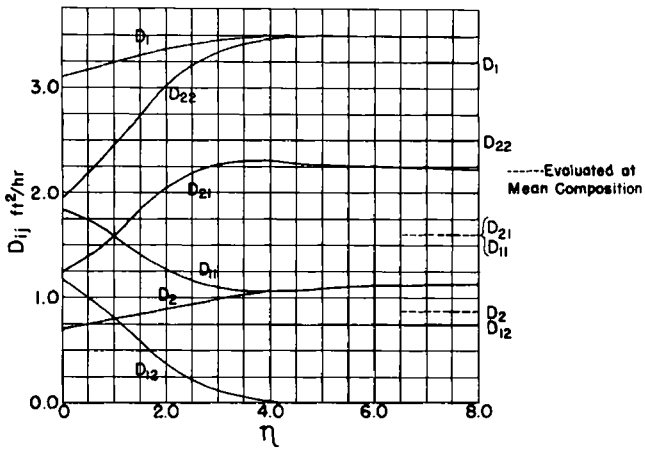

Fig. 7. Variation of D_{ij} with η.

$$\frac{\partial y_2}{\partial \theta} = \frac{\partial}{\partial z} D_{21} \frac{\partial y_1}{\partial z} + \frac{\partial}{\partial z} D_{22} \frac{\partial y_2}{\partial z} \qquad (12b)$$

The D_{ij} are given by Equation (2) and the boundary conditions by Equation (3*a*). The usual difference technique was used to represent these equations, and convergent solutions were found in the range of interest, $\theta > 0.5$ min., on a Control Data G21 computer. The numerical method was tested with constant diffusion coefficients and found to predict the analytic results to within 0.5%.

The numerical solutions obtained for the experimental conditions were within 0.5% of those predicted by the linearized theory; the two curves coincide in Figures 3 and 4.

This comparison provides another test of the Stefan-Maxwell Equations. Since the agreement is very close, well within the experimental error for all three runs, the results can be considered as additional support for the validity of the equations.

The numerical solutions to the ternary diffusion equations were also obtained for conditions other than those studied experimentally. Several sets of initial conditions were selected for study (*1*), one of which will be given here, experiment *BL2*. The initial conditions are less extreme than those studied experimentally, 0.6, 0.1, 0.3 for the top tube compositions for species 1, 2, and 3, respectively and 0.4, 0.5, and 0.1 for the bottom tube. It should be noted that the initial driving forces are similar in magnitude and it is therefore not clear which two species should be considered when using an effective diffusivity model.

In Figure 5 the numerical results are shown along with the two predictions possible with an effective diffusivity defined by Equation (11) (*1*). For each species one of the effective diffusivity calculations is quite close to the numerical results. Unfortunately different choices of components give the correct response for two different species. That is, one choice of components will predict the behavior of one species well, but not the other. A second choice may predict the second species, but not the first.

Table 5. Initial and Boundary Conditions

	$\eta = 0$ or $z = 0$			$\eta = \infty$ or $\theta = 0$		
Run	y_1	y_2	y_3	y_1	y_2	y_3
A	0.5	0.5	0	0	0.5	0.5
B	0.5	0.5	0	0.25	0.5	0.25
C	0.5	0.5	0	0.375	0.5	0.125

Table 6. Ternary Diffusivities (Sq. Ft./Hr.)

System	D_{11}	D_{12}	D_{21}	D_{22}
1	1.61	0.75	1.61	2.50
2	0.525	0.072	0.237	0.753
3	0.234	0.064	0.059	0.316

The linearized theory when $[D]$ is evaluated at the average composition again gives results within 0.5% of the numerical results and these results are indistinguishable from the numerical results in Figure 5.

A more severe test is to compare the concentration profiles in the diffusion tube obtained numerically to those predicted by the linearized equations [Equations (5), (5*a*), and (5*b*)]. The greatest deviation between the two solutions was obtained for times less than 10 min. Since in this range the penetration solution is valid, comparisons will be reserved for the next section.

PENETRATION SOLUTIONS

The numerical solutions to the ternary penetration problem [Equation (12) with the boundary conditions given by Equation (7)] were obtained by first reducing Equation (12) to two ordinary differential equations. The transformation used was the same as that of Kirkaldy et al. (*7*), $\eta = z/\sqrt{\theta}$, and the resulting equations were solved by a Runge-Kutta method. The concentration profiles obtained in this manner were compared with the numerical solution obtained previously for the bounded diffusion problem. The two solutions should be the same for short times before the effect of the wall influences the bounded results. Even though this is the most inaccurate region of the bounded numerical solution, the two solutions agreed to better than 0.5%. The Runge-Kutta method generally took less computer time than the numerical equations used to solve the experimental equations; both methods, however, required more than 30 min. for a complete analysis of a given experiment—thus the utility of the linearized theory.

Three different systems, shown in Table 4, were investigated with three different boundary conditions used (Table 5). The initial conditions were chosen so that the initial concentration difference of the lightest component, $y_3^I - y_3^o$, decreased from run *A* to *C*. In addition $y_2^I - y_2^o$ was chosen as zero for all runs so that the interaction effects could easily be detected.

The nitrogen-carbon dioxide-hydrogen system has binary diffusion coefficients comparable to those of the experimental system so that large interaction effects are to be

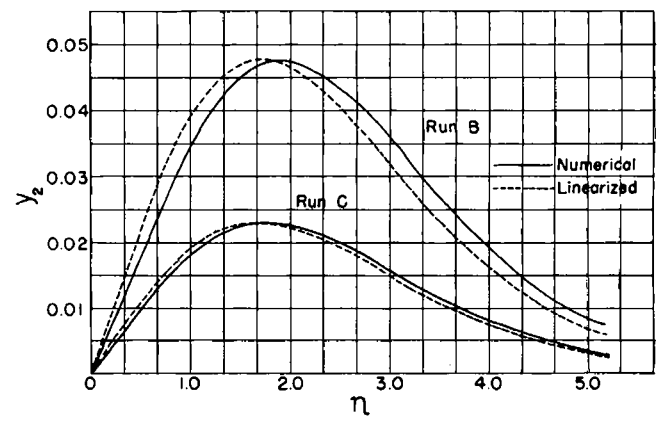

Fig. 8. Concentration profiles for component 2 in Semi-infinite system.

expected. The second and third systems, isopropanol-methanol-water and benzene-acetone-nitrogen, were chosen to give smaller interactions. The binary diffusion coefficients used are shown in Table 4.

The linearized predictions were made with Equations (8) and (9). Three compositions were used to evaluate $[D]$. An average composition was chosen as the linear average of the initial and boundary mole fractions for each species. As extremes, the initial and boundary mole fractions were also used to evaluate $[D]$. The concentrations as a function of η for the first system are shown in Figure 6 for species 2. The linearized solutions are shown along with the numerical solution. The two extreme linearized solutions are seen to bracket the solution which used the average $[D]$. A comparison of the numerical and the linearized solutions for species 2 (obtained with $[D]$ used at the average composition) shows that the concentration wave is shifted by the nonlinear terms in the numerical solution. The maximum amplitude of the numerical solution is essentially the same as that predicted by the linearized equations.

The local values of the elements and roots of $[D]$ are shown in Figure 7 as well as the values corresponding to the average composition.

When $y_3^I - y_3^o$ is decreased, the interaction effects become smaller and the curves for runs B and C tend to converge to the numerical solution. This is seen in Figure 8 for runs B and C. Only the linearized solutions obtained with the average composition used to evaluate $[D]$ are shown, since it is apparent from Figure 6 that this composition gives the best predictions. It should be noted that the concentration scale in Figure 8 is twice that of Figure 6.

The concentration profiles obtained for the second and third systems were similar to those obtained with the first system, but the differences between the numerical and linearized solutions decreased. The ternary coefficients evaluated at the average concentrations are given in Table 6 for all three systems. The fluxes at $z = 0$ calculated for the three systems may be conveniently tabulated as $\frac{\sqrt{\theta}}{C} N_i^I = \frac{1}{2}\int_o^\infty y_i(\eta)\,d\eta$. A comparison between the linearized and numerical results is shown in Table 7. The error shown in this table is the percent difference between the two solutions divided by the numerical value. Since the accuracy of the numerical solutions is estimated to be $\pm$ 0.0005, there is some uncertainty in these values. Although the concentration profiles given by the two methods tend to converge as the interactions decrease, the largest error in the flux does not occur in the system with the largest interactions. However, since the maximum error is less than 5%, these results, taken with earlier ones, indicate that the linearized equations of multicomponent mass transfer are sufficiently accurate for most engineering purposes.

Table 7. Tabulation of $\frac{\sqrt{\theta}}{C} N_i^I$

	Species 1			Species 2		
	I	II	III	I	II	III
System 1 Nitrogen-carbon dioxide-hydrogen						
Run *A*	0.3391	0.3333	1.7	0.1650	0.1651	−0.1
Run *B*	0.1762	0.1725	2.1	0.0741	0.0748	−0.9
Run *C*	0.0895	0.0880	1.7	0.0353	0.0349	+1.1
System 2 Isopropanol-methanol-water						
Run *A*	0.2034	0.2023	0.5	0.0439	0.0461	−4.8
Run *B*	0.1023	0.1031	0.7	0.0205	0.0210	−2.4
Run *C*	0.0513	0.0512	0.2	0.0099	0.0100	−1.0
System 3 Benzene-acetone-nitrogen						
Run *A*	0.1339	0.1321	1.3	0.0384	0.0400	−4.0
Run *B*	0.0681	0.0672	1.3	0.0178	0.0182	−2.2
Run *C*	0.0343	0.0343	0	0.0086	0.0087	−1.1

Column I. Predictions of the linearized theory when $[D]$ is evaluated at the average concentration.
Column II. Values obtained from numerical solutions.
Column III. Percent difference between I and II.

ACKNOWLEDGMENT

Acknowledgment is made to the donors of the Petroleum Research Fund, administered by the American Chemical Society, for partial support of this research, and to the financial support of the Shell Companies Foundation. The authors are grateful to Brian Horn for the numerical calculations in the bounded system.

NOTATION

C = molar density
$\mathcal{D}_{kj}$ = binary diffusivity
$\mathcal{D}_i$ = effective diffusivity
$[D]$ = diffusivity matrix
D_i = characteristic roots of $[D]$
(j) = column vector whose elements are molar flux vectors with respect to molar average velocity
L = length of diffusion tube
n = number of species
N_i = flux of species i
(N) = column vector with elements N_i
$\mathbf{V}^M$ = molar average velocity vector
V_z^M = z direction component of $\mathbf{V}^M$
y_i = mole fraction of species i
(y) = column vector whose elements are y_i
z = distance coordinate

Greek Letters

δ = Kronecker delta
η = $z/\sqrt{\theta}$
θ = time

Superscripts

$+$ = initial value in region $0 < z < L$
$-$ = initial value in region $-L < z < 0$
o = initial value
I = interfacial value
$\sim$ = mean value

LITERATURE CITED

1. Arnold, K. R., Ph.D. thesis, Carnegie Inst. Technol., Pittsburgh, Pa. (1965).
2. Boardman, L. E., and N. E. Weld, *Proc. Royal Soc. (London)*, **A162**, 511 (1937).
3. Chapman, S., and T. G. Cowling, "Mathematical Theory of Non-Uniform Gases," Cambridge Univ. Press, Cambridge (1939).
4. Cussler, E. L., Jr., and E. N. Lightfoot, *A.I.Ch.E. J.*, **9**, 783 (1963).
5. Fairbanks, D. F., and C. R. Wilke, *Ind. Eng. Chem.*, **42**, 471 (1950).
6. Jost, W., "Diffusion," Academic Press, New York (1952).
7. Kirkaldy, J. S., J. E. Lane, and G. R. Mason, *Can. J. Phys.*, **41**, 2174 (1963).
8. Stewart, W. E., and R. Prober, *Ind. Eng. Chem. Fundamentals*, **3**, 224 (1964).
9. Toor, H. L., *A.I.Ch.E. J.*, **10**, 448 (1964).
10. *Ibid.*, 460.
11. ———, C. V. Seshadri, and K. R. Arnold, *ibid.*, **11**, 746 (1965).
12. Wilke, C. R., *Chem. Eng. Progr.*, **46**, 95 (1950).

Manuscript received August 25, 1966; revision received January 12, 1967; paper accepted January 16, 1967.